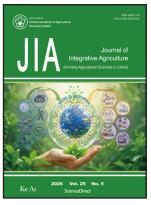
Journal of Integrative Agriculture 2026, 25(5): 2014–2027

Available online at ScienceDirect

Journal of Integrative Agriculture



RESEARCH ARTICLE

Free fatty acids induce apoptosis in mammary epithelial cells from ketotic dairy cows *via* endoplasmic reticulum stress

Renxu Chang[1, 2], Yuanyuan Chen[2], Xinyi Xu[3], Hongdou Jia[2], John Mauck[4], Juan J. Loor[4], Yehoshav A. Ben Meir[5], Qiushi Xu[2], Xudong Sun[2#], Chuang Xu[1#]

[1] *College of Veterinary Medicine, China Agricultural University, Beijing 100193, China*
[2] *Heilongjiang Provincial Key Laboratory of Prevention and Control of Bovine Diseases, College of Animal Science and Veterinary Medicine, Heilongjiang Bayi Agricultural University, Daqing 163319, China*
[3] *College of Arts and Sciences, University of North Carolina at Chapel Hill, Chapel Hill, NC 27514, USA*
[4] *Mammalian NutriPhysioGenomics, Department of Animal Sciences and Division of Nutritional Sciences, University of Illinois, Urbana 61801, USA*
[5] *Department of Ruminant Science, Institute of Animal Sciences, Agricultural Research Organization, Volcani Institute, Rishon LeTsiyon 750101, Israel*

Highlights

- Key Findings on Ketosis-Induced ER Stress: High concentrations of free fatty acid (FFA) in ketotic dairy cows activate endoplasmic reticulum (ER) stress pathways, contributing to mammary epithelial cell apoptosis and reduced milk yield.
- Clinical Relevance for Dairy Health: Findings highlight ER stress as a therapeutic target for mitigating metabolic stress-induced apoptosis in the mammary gland, offering potential strategies to improve dairy cows productivity.
- Future Implications: The study sets the stage for *in vivo* trials to validate ER stress inhibitors like Tauroursodeoxycholate (TUDCA) as practical solutions for managing ketosis and enhancing dairy cows health.

Abstract

The mammary glands of dairy cows with ketosis face unique challenges, including the supraphysiological circulating concentrations of free fatty acids (FFA) and apoptosis of epithelial cells. The fact that endoplasmic reticulum (ER) stress and apoptosis are closely related processes (at least in nonruminants) suggests that mechanisms of metabolic stress-induced apoptosis in bovine mammary epithelial cells may involve the ER stress pathway. The objective of this study was to investigate (1) the status of the ER stress pathway in mammary gland of dairy cows with ketosis, and (2) the role of ER stress in the apoptosis of bovine mammary epithelial cells challenged with high concentrations of FFA. Ketosis or exogenous FFA activated the ER stress pathway in the mammary gland of dairy cows or MAC-T cells. Pretreatment with the ER stress activator Tunicamycin (Tun) aggravated ER stress and apoptosis in MAC-T cells induced by FFA. However, ER stress inhibitor Tauroursodeoxycholate (TUDCA) attenuated ER stress induced by FFA and also attenuated the apoptosis in MAC-T cells. In conclusion, the data confirmed that FFA induced apoptosis of bovine mammary epithelial cells in dairy cows with ketosis *via* ER stress signaling. Thus, timely resolution of ER stress may help counteract the negative effects of ketosis on the mammary gland.

Keywords: ketosis, bovine mammary epithelial cells, ER stress, apoptosis

1. Introduction

Ketosis is one of the most common metabolic disorders in dairy cows during the peripartum period (Gu *et al*. 2021). The high incidence of ketosis in dairy cows has been ascribed to a state of negative energy balance induced by metabolic stress, which is characterized by high and sustained free fatty acid (FFA) concentrations in the circulation (Ruprechter *et al*. 2011). High plasma FFA are primarily used by the liver with a resultant increase of ketone body production and export into the blood (Miles *et al*. 2022). Supraphysiological

Received 20 February 2024; Received in revised form 21 August 2024; Accepted 4 December 2024; Available online 24 December 2024
Renxu Chang, E-mail: changrenxv@163.com; #Correspondence Xudong Sun, E-mail: sunxudong0323@163.com; Chuang Xu, E-mail: xuchuang@cau.edu.cn; xuchuang7175@163.com

© 2026 CAAS. Publishing services by Elsevier B.V. on behalf of KeAi Communications Co. Ltd. This is an open access article under the CC BY-NC-ND license (http://creativecommons.org/licenses/by-nc-nd/4.0/). Peer review under responsibility of Editorial Board of *Journal of Integrative Agriculture*.
doi: 10.1016/j.jia.2024.12.023

concentrations of ketone bodies and the subsequent ketosis causes huge economic losses in dairy industry.

The major economic losses caused by ketosis are mainly attributable to reduced milk yield (Bauer and Jagusiak 2022). Excessive apoptosis leads to a decline in the number of functional cells in the mammary gland of dairy cows (Wang and Song 2018). Our previous study with ketotic dairy cows revealed an activation of apoptosis in mammary epithelial cells and a subsequent decrease in milk yield (Sun *et al.* 2021; Chang *et al.* 2023). The underlying signaling mechanisms of metabolic stress-activated apoptotic processes in bovine mammary epithelial cells have not been fully elucidated.

In eukaryotic cells, the endoplasmic reticulum (ER) is essential for processing, modifying, and assembling proteins, all of which are strictly regulated and affect the fate and function of the cell (Zhao *et al.* 2013; Li *et al.* 2019; Mo *et al.* 2023). The imbalance between unfolded proteins that enter the ER and the ability of ER to fold and export proteins results in ER stress, which leads to physiological dysfunction in cells (Waldherr *et al.* 2019; Xu *et al.* 2021). Persistent ER stress is also closely related to apoptosis (Papandreou *et al.* 2015; Lu *et al.* 2022). At least in nonruminants, ER stress was activated by metabolic stress and the persistent ER stress subsequently resulted in hepatic cell apoptosis (Nasiri-Ansari *et al.* 2021; Moslehi *et al.* 2023). It is noteworthy that ER stress and increased cell apoptosis characterize the mammary gland and liver in dairy cows undergoing metabolic disorders (Zhu *et al.* 2019; Chang *et al.* 2023). Thus, in light of the close relationship, ER stress might play a main role in metabolic stress-induced apoptosis of bovine mammary epithelial cells.

Although there are some studies highlighting that apoptosis can be induced by persistent ER stress in nonruminants, it is unclear whether apoptosis in mammary gland of dairy cows with ketosis is associated with ER stress. The primary objective of this study was to assess ER stress status in the mammary gland of dairy cows with ketosis and the role of ER stress in FFA-induced apoptosis of bovine mammary epithelial cells were investigated.

2. Materials and methods

2.1. Animals, diets and sampling

Lactating cows with same parity (median=3, range=2–4) and similar days in milk (median=6, range=3–10) from a commercial 2,000-head dairy farm located in Daqing City (Heilongjiang Province, China) were housed individually in a room with solid wooden floor pens. The dairy cows used in this study were Holstein dairy cows with body weights ranging from 600 to 650 kg. During the experiment, the cows were housed in a temperature-controlled room, with the temperature maintained at 20°C–22°C and humidity at 50–60%. Dairy cows were fed twice a day at 8:00 am and 16:00 pm with the same total mixed ration (TMR) and had free access to water. The nutritional composition and formulae of feed are shown in Table 1. This TMR diet was formulated to meet the nutritional requirements for lactating Holstein cows, as recommended by the National Research Council (NRC 2021). The ration provides sufficient energy, protein, and minerals to support milk production, maintain body condition, and ensure reproductive health (Van Soest *et al.* 1991; Saun 2022). The calculated net energy for lactation (NEL) of 6.70 MJ kg^{-1} is appropriate for cows with moderate milk production levels. Dairy cows with other clinical illnesses were screened out by 2 experienced veterinarians. Ketosis was preliminarily identified using a portable meter (TNN-2, Yicheng Bioelectronics Technology Co., Ltd., China) to measure the blood β-hydroxybutyric acid (BHB) concentrations. If dairy cows had a positive nitroprusside test and reduced milk yield, feed intake, or both that was accompanied by BHB concentrations greater than 3 mmol L^{-1}, veterinarians classified them as suspected clinically ketotic. If dairy cows had no visible clinical symptoms accompanied by BHB concentrations lower than 0.6 mmol L^{-1}, veterinarians classified them as healthy. This approach led to 65 dairy cows identified by the ketone powder method combined with BHB quantitative determination as being positive or negative for hyperketonemia: 22 as suspected ketotic or 43 as healthy. Blood was collected for 3 consecutive days from the tail vein before the morning feeding, and centrifuged at 3,500×g for 15 min at 4°C to obtain serum. The serum levels of glucose, BHB and FFA were measured in a Hitachi 7,170 autoanalyzer (Hitachi, Tokyo, Japan) with glucose (GL3815, Randox Laboratories), BHB (RB1008 Randox Laboratories, Crumlin, UK) and FFA (FA115, Randox Laboratories) Assay Kits. In Exp. 1, based on the serum biochemical indices (Li *et al.* 2022), the final sample included 20 dairy cows: 10 healthy (CON) cows (BHB concentration<0.6 mmol L^{-1},

Table 1 Ingredient and nutrient composition of the diets (Exp. 1)

Ingredient (% of dry matter)	
Corn silage	40.00
Corn	35.00
Wheat bran	8.00
Sunflower	8.00
Soybean meal	5.00
Premix[1)]	0.60
Limestone ($CaCO_3$)	0.90
Dicalcium phosphate ($CaHPO_4$)	0.30
$NaHCO_3$	1.20
NaCl	1.00
Total	100.00
Nutrient composition (% of dry matter)	
Non-fiber carbohydrate	40.40
Neutral detergent fiber	33.45
Acid detergent fiber	17.20
Crude protein	15.20
NEL (MJ kg^{-1})[2)]	6.70
Ca	0.70
P	0.50

[1)] Provided per kilogram of TMR: vitamin E (as dl-alpha-tocopherol acetate) 18 IU, vitamin D (as cholecalciferol) 1,260 IU, vitamin A (as retinyl acetate) 3,600 IU, Co (as cobalt sulfate) 0.126 mg, I (as potassium iodide) 0.108 mg, Mn (as manganese sulfate) 23.4 mg, Cu (as cobalt carbonate) 10.8 mg, Fe (as iron sulfate) 36 mg, Zn (as zinc sulfate) 43.2 mg, Se (as sodium selenite) 0.23 mg.
[2)] NEL was a calculated value and others were measured values.

FFA concentration<0.4 mmol L^{-1}, and glucose>3.5 mmol L^{-1} without clinical symptoms) and 10 clinically ketotic (CK) cows (BHB concentration>3 mmol L^{-1}, FFA concentration>0.5 mmol L^{-1}, and glucose<3.5 mmol L^{-1}). The CK cows had a decreased feed intake, rapid loss of body weight, excessively dry feces, and decreased milk yield. An automatic milking system was used to record milk yield. The DMI was calculated by multiplying the DM content of the TMR with daily feed intake (the difference between the offered and actual feed intake). Each cow was assessed by three skilled veterinarians using a body condition score (BCS) that ranged from 1 to 5 in increments of 0.25 (Montevecchio *et al.* 2023). Table 2 displays the physiological data of the dairy cows that were utilized. The mammary gland tissue biopsy was performed as reported in our previous study (Sun *et al.* 2021). Briefly, after administration of local anesthesia, a mammary biopsy was collected from the left rear quarter in each dairy cow (10 in CON or CK) and stored in liquid nitrogen for subsequent experiments.

2.2. Cell culture and treatment

Bovine mammary epithelial cells (MAC-T) were purchased from Shanghai Shunran Biology. MAC-T cells were cultured in growth medium (DMEM/F12 (Grand Island, New York, USA)+growth-promoting hormone (1 mg L^{-1} progesterone (5341, Sigma-Aldrich, St. Louis, MO), 0.05% α lactose (HY-N2514, MedChem Express, Monmouth Junction, NJ), and 0.05% lactalbumin (L5385, Sigma-Aldrich)+10% fetal bovine serum (FB15015, Clark Bioscience, USA)+1% antibiotic–antimycotic mix (HyClone, South Logan, UT, USA)+10 μg L^{-1} insulin (Sigma-Aldrich)) in 5% CO_2 incubator at 37°C according to the previous study (Chang *et al.* 2022). The cells were passaged at approximately 80% confluence as needed, and the growth medium was changed daily. Approximately 24 h before applying treatments, the cells were cultured in a lactogenic medium (DMEM/F-12+2.5 mg L^{-1} prolactin (100–07, Peprotech, Rocky Hill, NJ)+1 g L^{-1} BSA (4240GR500, BioFROXX, Beijing, China)).

In Exp. 2, different FFA concentrations were used to simulate hyperlipidemia in ketotic cows. A 52.7 mmol L^{-1} FFA mixture was prepared as previously described (Sun *et al.* 2019). Briefly, 22.9 mmol L^{-1} oleic acid (O1383, Sigma-Aldrich), 7.6 mmol L^{-1} stearic acid (S4751, Sigma-Aldrich), 2.6 mmol L^{-1} linoleic acid (L1012, Sigma-Aldrich), 16.8 mmol L^{-1} palmitic acid (P5585, Sigma-Aldrich), and 2.8 mmol L^{-1} palmitoleic acid (P9417, Sigma-Aldrich) were dissolved at 60°C in 0.1 mol L^{-1} KOH and hydrochloric acid used to adjust pH to 7.4. The FFA were heated in a 60°C water bath until fully clear, then rapidly introduced into RPMI-1640 medium containing 2% BSA, followed by incubation at 37°C for 30 min to enable the formation of BSA-FFA complexes. There were 4 experimental treatments: 0 mmol L^{-1} FFA, 2% BSA was used to treat cells for 24 h; 0.6 mmol L^{-1} FFA, 0.6 mmol L^{-1} FFA was used to treat cells for 24 h; 1.2 mmol L^{-1} FFA, 1.2 mmol L^{-1} FFA was used to treat cells for 24 h; 2.4 mmol L^{-1} FFA, 2.4 mmol L^{-1} FFA was used to treat cells for 24 h. After the treatment period, the MAC-T cells were collected and prepared for subsequent analysis. The cells were harvested, washed with PBS, and then either lysed for protein extraction or fixed for immunofluorescence staining, depending on the specific analysis required. Each treatment group was performed in triplicate to ensure the reliability of the results.

In Exp. 3, to explore the role of ERs activation in FFA-induced apoptosis, 2 mg of Tunicamycin (Tun; HY-A0098, MedChem Express, Monmouth Junction, NJ) was dissolved with dimethyl sulfoxide (DMSO; (1.0 mL) D8371, Solarbio, Beijing, China) to generate the stock solution (2 mg mL^{-1}). There were 4 experimental treatments: BSA+DMSO, DMSO was used to treat cells for 12 h prior to addition of 2% BSA for an additional 24 h; 1.2 mmol L^{-1} FFA+DMSO, DMSO was used to treat cells for 12 h prior to challenge with 1.2 mmol L^{-1} FFA for 24 h; BSA+2 μg mL^{-1} Tun, 2 μg mL^{-1} Tun was used to treat cells for 12 h prior to addition of 2% BSA for an additional 24 h; FFA+2 μg mL^{-1} Tun, 2 μg mL^{-1} Tun was used to treat cells for 12 h prior to challenge with 1.2 mmol L^{-1} FFA for an additional 24 h. Following treatment, the cells were harvested for various analyses, including immunofluorescence staining to detect ER stress markers and flow cytometry to assess the rate of apoptosis. Each treatment group was performed in triplicate to ensure the reliability of the results. A 2×2 factorial design was used, with Factor A representing the presence or absence of Tun, and Factor B indicating the presence or absence of FFA.

In Exp. 4, to explore the role of ERs inhibition in FFA-induced apoptosis, 500 mg Tauroursodeoxycholate (TUDCA; HY-19696, MedChem Express) was dissolved with DMSO (1.0 mL) to generate the 100 mmol L^{-1} stock solution. There were 4 experimental treatments: BSA+DMSO, DMSO was used to treat cells for 12 h prior to addition of 2% BSA for an additional 24 h; 1.2 mmol L^{-1} FFA+DMSO, DMSO was used to treat cells for 12 h prior to challenge with 1.2 mmol L^{-1} FFA for 24 h; BSA+200 μmol L^{-1} TUDCA, 200 μmol L^{-1} TUDCA was used to treat cells for 12 h prior to addition of 2% BSA for an additional 24 h; FFA+200 μmol L^{-1} TUDCA, 200 μmol L^{-1} TUDCA was used to treat cells for 12 h prior to challenge with 1.2 mmol L^{-1} FFA for an additional 24 h. Post-treatment, cells were collected for protein extraction and Western blot analysis to quantify the expression of proteins involved in apoptosis and ER stress pathways. Each treatment group was performed in triplicate to ensure the reliability of the results. A 2×2 factorial design was utilized, with Factor A represented the presence or absence of TUDCA, and Factor B indicated the presence or absence of FFA.

Table 2 Basic description of Holstein cows classified as healthy (CON) or having clinical ketosis (CK) (Exp. 1, *n*=10)

Item	Median (IQR)[1)]	
	CON	CK
DMI (kg d^{-1})	20.48 (3.43)	18.45 (4.38)*
BCS	2.88 (0.75)	3.63 (0.56)*
Milk yield (kg)	43.66 (4.45)	36.87 (5.27)*
Serum BHB (mmol L^{-1})	0.90 (0.53)	3.55 (0.42)*
Serum FFA (mmol L^{-1})	0.29 (0.08)	1.01 (0.22)*
Serum glucose (mmol L^{-1})	4.00 (0.85)	(0.20)*

[1)] IQR, interquartile range.
*, P<0.05 within a row denote differences.

2.3. Immunofluorescence staining (Exps. 3 and 4)

The MAC-T cells were grown on laser confocal petri dishes

for 24 h and then fixed for 30 min using 4% paraformaldehyde followed by washed 3 times with PBS. The samples were blocked with protease K (U8805, TIANGEN, Beijing, China) working solution for 30–40 s. To remove excess protease K, cells were then washed 3 times with PBS. Triton X-100 (0.3%, P0096, Beyotime Biotechnology, Shanghai, China) was used to increase the permeability of cells. Subsequently, the cells were incubated with the cytokeratin 18 primary antibody (1:100; ab133263, Abcam, Cambridge, MA) in goat serum (AR0009, BOSTER Biological Technology Co., Ltd., Wuhan, China) at 4°C overnight. The FITC-conjugated goat antirabbit immunoglobulin G second antibody (BA1105, BOSTER Biological Technology Co., Ltd.) was added at room temperature for 30 min. The cells were then incubated with DAPI (D9542, Sigma-Aldrich) for staining of nuclei after washing with PBS. Excess DAPI was eliminated with 3 washes of PBS. The fluorescence of samples was imaged using confocal microscopy and quantified by Image J software. The fluorescence density of caspase 3 was quantified by mean density (mean staining intensity=integrated optical density sum/area sum).

2.4. Flow cytometry assay (Exps. 3 and 4)

Annexin V-FITC Apoptosis Detection Kit (C1062L, Beyotime Biotechnology) were used to identify apoptosis. After processed as mentioned above, cells were harvested with EDTA-free trypsin and terminated with the original medium. The cell suspension was centrifuged to discard culture medium and simultaneously stained with 10 μL PI (red fluorescence) and 5 μL Annexin V-FITC (green fluorescence) at room temperature protected from light for 12 min. Flow cytometry was then used to detect apoptotic cells.

2.5. Protein extraction and Western blotting (Exps. 1, 2, 3 and 4)

To prepare protein samples for Western blotting, total protein from mammary gland tissue of dairy cows and MAC-T cells were extracted using PMSF (P0100, Solarbio)-containing RIPA (R0020, Solarbio) buffer. The concentrations of protein were determined using a BCA protein concentration assay kit (P0009, Beyotime Biotechnology). Equal amounts of lysate protein were electrophoresed in SD-PAGE to separate protein bands. The protein was transferred to polyvinylidene difluoride (PVDF) membranes (Merck Millipore, Billerica, MA, USA) using transblot equipment. After blocking with 5% non-fat milk (232100, BD, Franklin Lakes, NJ), the PVDF membranes were incubated with primary antibodies raised against the protein of interest. The primary antibodies were as follows: glucose regulated protein 78 (GRP78; 1:1,000; 11,587, Proteintech Group, Inc., Beijing; China), activated transcription factor 6 (ATF6; 1:1,000; ab122891, Abcam), p-inositol requiring enzyme (p-IRE1; 1:1,000; PA116927, Invitrogen, Carlsbad, CA, USA), IRE1 (1:1,000; 3294T, Cell Signaling Technology, Danvers, MA), p-protein kinase RNA-like endoplasmic reticulum kinase (p-PERK; 1:1,000; ab192591, Abcam), PERK (1:1,000; 3192S, Cell Signaling Technology), C/EBP homologous protein (CHOP; 1:1,000; 15204-1, Proteintech Group, Inc.), caspase 9 (1:1,000, 10380-1-AP, Proteintech Group, Inc.), caspase 3 (1:1,000; A2156, ABclonal Technology, Wuhan, China), B-cell lymphoma 2 (Bcl2; 1:1,000; 12789, Proteintech Group, Inc.), BCL-2-associated X protein (Bax; 1:1,000; 50599, Proteintech Group, Inc.), β-actin (1:1,000; M20011S, Abmart, Shanghai, China). Excess primary antibody was removed by washed with 1× TBST, and the PVDF membranes then incubated with goat anti-mouse (1:5,000; BA1050, BOSTER Biological Technology Co., Ltd.) or rabbit (1:5,000; BA1054, BOSTER Biological Technology Co., Ltd.) secondary antibody for 45 min in room temperature. The PVDF membranes were developed with an Enhanced Chemiluminescence Solution Detection Kit (ECL, Merck Millipore) reagent and photographed with a gel-imaging system (Protein Simple, Santa Clara, CA, USA) after washing with TBST. The protein bands were analyzed using Image Lab software (Bio-Rad Laboratories, Inc.).

2.6. Statistical analyses

At least 3 independent experiments were conducted with all data, and SPSS 23.0 software (IBM Corp., Armonk, NY) was used for analysis. The Shapiro-Wilk test was used to verify that the data was normal. Whereas normally distributed data are expressed as means±standard error (SE), non-normally distributed data are reported as median (interquartile range). For Exp. 1, the Mann-Whitney U test was used to analyze differences in nonparametric variables with a skewed distribution. For normally distributed data, unpaired Student's *t*-test used when comparing 2 groups. Dairy cow was the experimental unit. For Exp. 2, the one-way ANOVA was used to analyze the effect of FFA. Linear and quadratic contrasts were used to evaluate dose-dependent effects. As for Exps. 3 and 4, two-way ANOVA was employed to assess the main effects of each factor and their interaction on the dependent variables. When there was a significant effect, one-way ANOVA method was used to test the differences among means. For Exps. 2–4, the cell was considered the experimental unit. Differences with $P<0.05$ were considered to indicate statistical significance.

3. Results

3.1. Baseline characteristics of the ketotic cows (Exp. 1)

Compared with CON, the DMI ($P=0.023$) was lower and the BCS ($P=0.009$) was greater in dairy cows with CK (Table 2). Compared with CON, dairy cows in the CK group had lower milk yield ($P<0.0001$, Table 2). The serum concentrations of BHB ($P<0.0001$) and FFA ($P<0.0001$) were greater, while serum concentration of glucose ($P<0.0001$) was lower in the CK group (Table 2).

3.2. ER stress status in the mammary glands of ketotic cows (Exp. 1)

Compared with CON, the protein abundances of GRP78 ($P<0.0001$, Fig. 1-A and B) and ATF6 ($P<0.0001$, Fig. 1-A and C) were greater in the mammary glands of dairy cows in the CK group. In addition, compared with CON, the ratios of p-IRE1/IRE1 ($P<0.0001$, Fig. 1-A and D) and p-PERK/PERK ($P<0.0001$, Fig. 1-A and E) and the protein abundance of

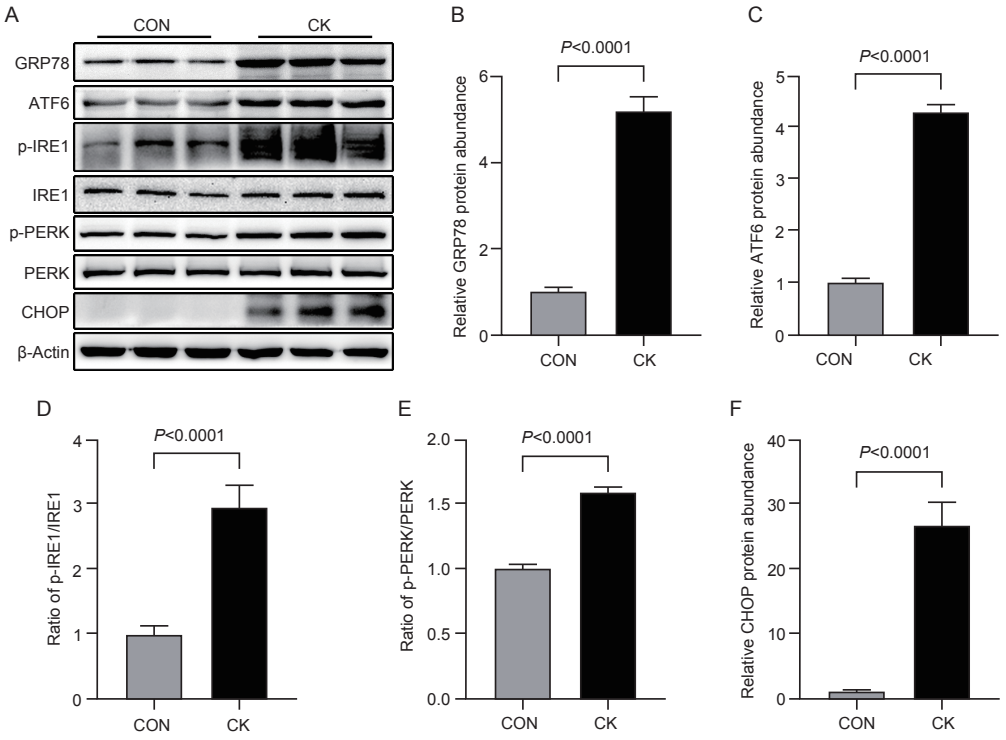


Fig. 1 Endoplasmic reticulum (ER) stress status in the mammary glands of ketotic cows (Exp. 1). A, Western blot image of GRP78, ATF6, p-IRE1, IRE1, p-PERK, PERK, CHOP, and β-actin. B, C and F, relative protein abundance of GRP78 (B), ATF6 (C) and CHOP (F). D and E, ratio of p-IRE1/IRE1 (D) and p-PERK/PERK (E). CK, clinical ketosis; CON, healthy cows. Data are mean±SEM (n=10).

CHOP (P<0.0001, Fig. 1-A and F) were greater in mammary gland of CK dairy cows.

3.3. FFA induced ER stress in MAC-T cells (Exp. 2)

The validity of MAC-T cells as a model was first verified using cytokeratin 18 staining before subsequent experiments (Fig. 2-A). As demonstrated in Fig. 2-B and C, the protein abundance of GRP78 in 1.2 mmol L^{-1} (P=0.013) and 2.4 mmol L^{-1} (P<0.0001) FFA-treated MAC-T cells were greater than that in 0 mmol L^{-1} FFA-treated cells (linear). Treatment with 0.6 (P=0.014), 1.2 (P=0.0049), or 2.4 mmol L^{-1} (P<0.0001) FFA increased the abundance of ATF6 protein in MAC-T cells (linear and quadratic, Fig. 2-B and D). Compared with 0 mmol L^{-1}, the ratio of p-IRE1/IRE1 was greater in the 1.2 mmol L^{-1} treatment group (quadratic, P=0.0002, Fig. 2-B and E), while the ratio of p-PERK/PERK was greater in the 0.6 (P=0.038), 1.2 (P<0.0001), and 2.4 mmol L^{-1} (P<0.0001) treatment groups (linear, Fig. 2-B and F). Furthermore, the CHOP protein abundance was greater after treatment with 1.2 or 2.4 mmol L^{-1} FFA (linear and quadratic, P<0.0001, Fig. 2-B and G).

3.4. Tunicamycin aggravated FFA-induced ER stress in MAC-T cells (Exp. 3)

The statistical analysis revealed that both FFA and Tun had significant main effects on the protein abundance of GRP78 (P<0.0001, Fig. 3-A and B). Additionally, significant main effects of FFA and Tun were observed on the protein abundance of ATF6 and the ratio of p-IRE1/IRE1 (P<0.0001, Fig. 3-A, C and D). Notably, the interaction effect between FFA and Tun was also significant (P<0.0001, Fig. 3-A, C and D). Compared with those in the DMSO group, the protein abundances of ATF6 (P=0.0002, Fig. 3-A and C) and the ratio of p-IRE1/IRE1 (P=0.014, Fig. 3-A and D) were greater in the Tun group. In addition, pretreatment with Tun aggravated the upregulation of ATF6 (P<0.0001, Fig. 3-A and C) protein abundance and the ratio of p-IRE1/IRE1 (P<0.0001, Fig. 3-A and D) that was induced by FFA. Furthermore, a significant main effect of FFA was found on the ratio of p-PERK/PERK and the protein abundance of CHOP (P<0.0001), while Tun also demonstrated a significant effect (P<0.0001, Fig. 3-A, E and F).

3.5. Activation of ER stress aggravated FFA-induced apoptosis in MAC-T cells (Exp. 3)

The results showed that FFA had a significant main effect on cleaved-caspase 9 and cleaved-caspase 3 protein abundance, and the ratio of Bax/Bcl2 (P<0.0001), while Tun also demonstrated a significant effect (P<0.0001, Fig. 4-A–D). Importantly, there was a significant interaction between FFA and Tun (P<0.0001), indicating that the effect of FFA on cleaved-caspase 9 and cleaved-caspase 3 protein abundance, and the ratio of Bax/Bcl2 depended on the level of Tun. Specifically, compared with DMSO, the cleaved-caspase 9 protein abundance (P<0.0001, Fig. 4-A and B) and the ratio of Bax/Bcl2 (P=0.0005, Fig. 4-A and D) were

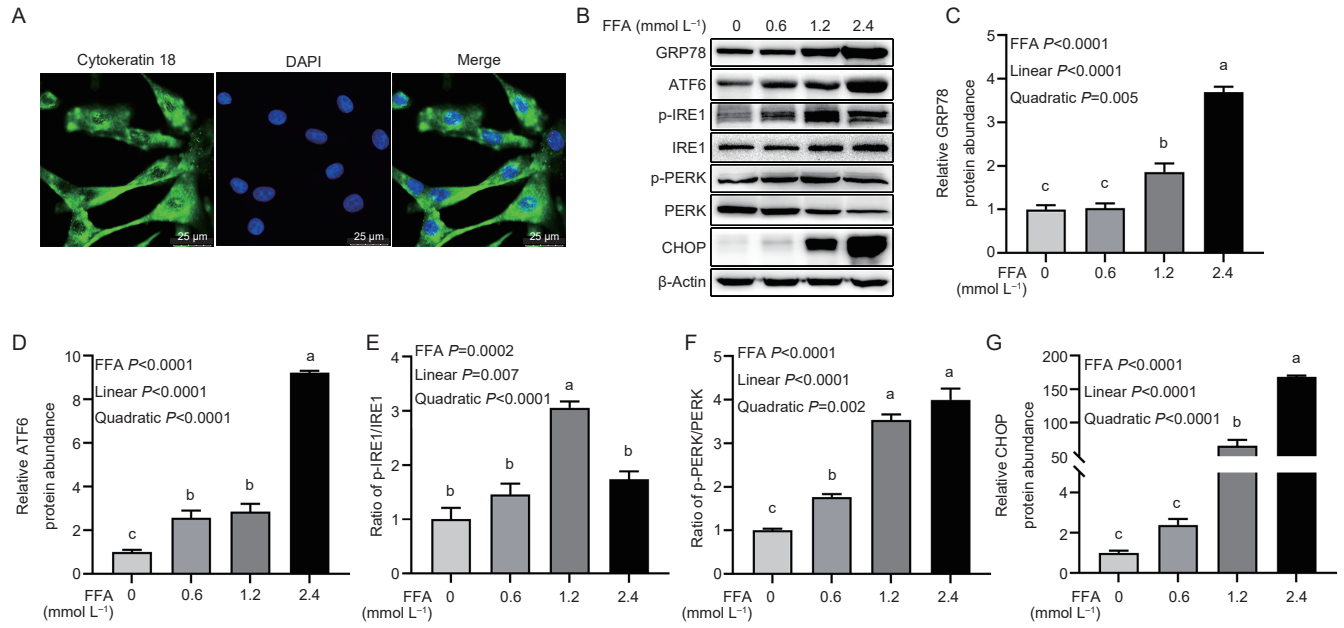


Fig. 2 Free fatty acids (FFA) induced endoplasmic reticulum (ER) stress in immortalized bovine mammary epithelial cells (MAC-T) (Exp. 2). MAC-T cells were treated with 0, 0.6, 1.2, and 2.4 mmol L^{-1} FFA for 24 h. A, representative cytokeratin 18 immunofluorescence staining images of MAC-T cells. B, Western blot image of GRP78, ATF6, p-IRE1, IRE1, p-PERK, PERK, CHOP, and β-actin. C, D and G, relative protein abundance of GRP78 (C), ATF6 (D) and CHOP (G). E and F, ratio of p-IRE1/IRE1 (E) and p-PERK/PERK (F). Data are mean±SE (n=3). Different letters indicate a significant difference (P<0.05).

greater in MAC-T cells pretreated with Tun. Compared with DMSO+FFA, the protein abundance of cleaved-caspase 9 (P<0.0001, Fig. 4-A and B), cleaved-caspase 3 (P<0.0001, Fig. 4-A and C) and the ratio of Bax/Bcl2 (P<0.0001, Fig. 4-A and D) were greater in Tun+FFA. Consistent with alterations at the protein level, the two-way ANOVA similarly identified significant main effects of both FFA and Tun on the fluorescence density of caspase 3 (P<0.0001, Fig. 4-E and F). Furthermore, FFA has significant main effect on apoptosis (P<0.0001), with Tun similarly showing a significant effect (P=0.015, Fig. 4-G and H).

3.6. Tauroursodeoxycholate attenuated FFA-induced ER stress in MAC-T cells (Exp. 4)

The results revealed a significant main effect of FFA on the protein abundance of GRP78 (P<0.0001), with TUDCA also showing a notable main effect (P=0.001, Fig. 5-A and B). Furthermore, significant main effects of both FFA and TUDCA were observed on the protein abundance of ATF6 and the ratio of p-IRE1/IRE1 (P<0.0001, Fig. 5-A, C and D). Notably, the interaction effect between FFA and TUDCA was also significant (P<0.0001, Fig. 5-A, C and D). Compared with DMSO, protein abundances of ATF6 (P<0.0001, Fig. 5-A and C) and the ratio of p-IRE1/IRE1 (P<0.0001, Fig. 5-A and D) were greater in response to 1.2 mmol L^{-1} FFA treatment. However, pretreatment with TUDCA, an inhibitor of ER stress, decreased protein abundance of ATF6 (P<0.0001) along with attenuating the upregulation of ATF6 protein abundance (P<0.0001) and p-IRE1/IRE1 (P<0.0001) induced by FFA (Fig. 5-A, C and D). In addition, the ratio of p-PERK/PERK showed a significant main effect due to FFA (P<0.0001), and TUDCA also demonstrated a significant effect (P<0.0001, Fig. 5-A and E). Both FFA and TUDCA had significant main effects on the protein abundance of CHOP (P<0.0001, Fig. 5-A and F), with the interaction between them was significant (P<0.0001, Fig. 5-A and F). Compared with DMSO, protein abundances of CHOP (P<0.0001, Fig. 5-A and F) were greater in response to 1.2 mmol L^{-1} FFA treatment. However, pretreatment with TUDCA attenuated the upregulation of CHOP protein abundance induced by FFA (P<0.0001, Fig. 5-A and F).

3.7. Inhibition of ER stress attenuated apoptosis in MAC-T cells induced by FFA (Exp. 4)

The analysis revealed a significant main effect of FFA on cleaved-caspase 9 (P<0.0001), with TUDCA also showing a significant main effect (P=0.01), and a notable interaction between FFA and TUDCA was identified (P<0.0001, Fig. 6-A and B). The cleaved-caspase 9 (P<0.0001) was greater after FFA treatment compared with DMSO (Fig. 6-A and B). In contrast, inhibition of ER stress by TUDCA attenuated the upregulation of the cleaved-caspase 9 (P=0.0005) induced by FFA (Fig. 6-A and B). Furthermore, both of FFA and TUDCA had a significant main effect on cleaved-caspase 3 protein abundance and the Bax/Bcl2 ratio (P<0.0001), with the interaction between FFA and TUDCA was also significant (P<0.0001, Fig. 6-A, C and D). Compared with DMSO, protein abundances of cleaved-caspase 3 (P<0.0001) and the ratio of Bax/Bcl2 (P<0.0001) were greater after FFA treatment (Fig. 6-A, C and D). In contrast, inhibition of ER stress by TUDCA attenuated the upregulation of the cleaved-caspase 3 (P<0.0001) protein abundance and the ratio of

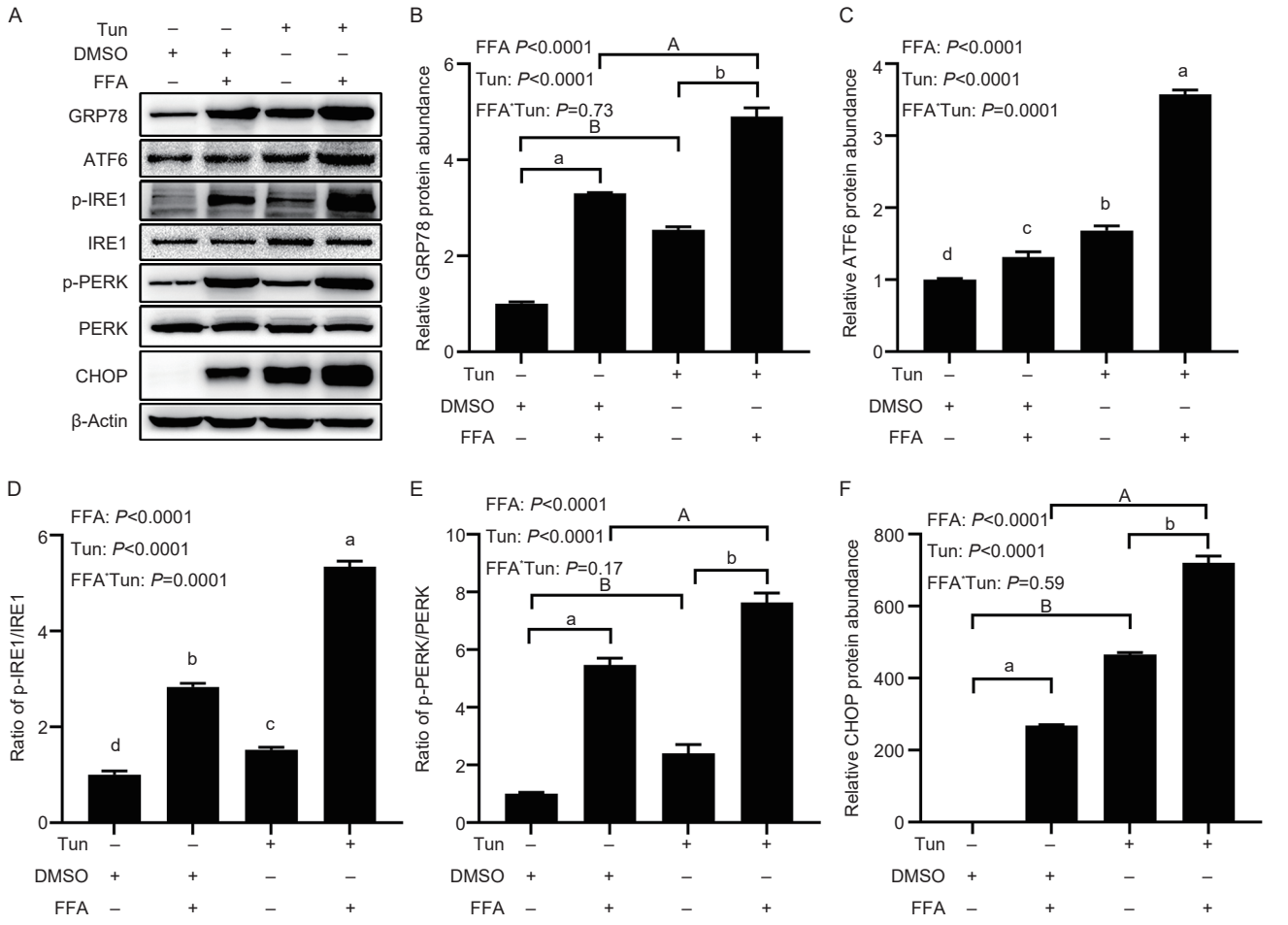


Fig. 3 Tunicamycin (Tun) aggravated free fatty acids (FFA)-induced endoplasmic reticulum (ER) stress in MAC-T cells (Exp. 3). MAC-T cells were pretreated with dimethyl sulfoxide (DMSO) or Tun for 12 h and treated with 0 or 1.2 mmo L^{-1} FFA in 2% BSA medium for another 24 h. A, Western blot image of GRP78, ATF6, p-IRE1, IRE1, p-PERK, PERK, CHOP, and β-actin. B, C and F, relative protein abundance of GRP78 (B) ATF6 (C) and CHOP (F). D and E, ratio of p-IRE1/IRE1 (D) and p-PERK/PERK (E). Data are mean±SE (n=3). Different letters in single bars indicate a significant difference (P<0.05) determined by their interaction. Different uppercase letters in paired bars indicate significant differences (P<0.05) between Tun-treated and non-treated groups, as determined by the main effect of Tun. Different lowercase letters in paired bars indicate significant differences (P<0.05) between FFA-treated and non-treated groups, as determined by the main effect of FFA.

Bax/Bcl2 (P<0.0001) induced by FFA (Fig. 6-A, C and D). Similarly, FFA significantly impacted the relative fluorescence density of caspase 3 (P<0.0001) and the apoptosis of MAC-T cells (P<0.0001). TUDCA similarly had a significant main effect on both the relative fluorescence density of caspase 3 (P<0.0001) and the apoptosis of MAC-T cells (P=0.006, Fig. 6-E–H). The interaction effect between FFA and TUDCA was also significant for both the relative fluorescence density of caspase 3 (P<0.0001) and the apoptosis of MAC-T cells (P=0.025, Fig. 6-E–H). Compared with DMSO, the relative fluorescence density of caspase 3 was greater in MAC-T cells with FFA (P<0.0001), but it was attenuated by TUDCA pretreatment (P<0.0001, Fig. 6-E and F). In addition, the apoptosis of MAC-T cells was increased upon FFA treatment (P<0.0001, Fig. 6-G and H), but it was attenuated by TUDCA pretreatment (P=0.011, Fig. 6-G and H).

4. Discussion

The results of this study partially support the hypothesis that FFA-induced ER stress contributes to apoptosis in the mammary epithelial cells of ketotic cows. Treatment with FFA led to increased activation of the ER stress pathway, as evidenced by elevated levels of key ER stress markers and a corresponding increase in cell apoptosis. The use of the ER stress activator Tun further exacerbated this response, while the inhibitor TUDCA effectively mitigated both ER stress and apoptosis. This suggests that ER stress is a critical mediator in FFA-induced apoptosis. These findings underscore the importance of managing ER stress in mitigating ketosis-related damage to mammary gland health and provide a basis for developing targeted interventions in dairy cow management. However, certain aspects of the hypothesis were not fully supported. For instance, although FFA induced ER stress, the expected synergistic interaction between FFA and Tun was less evident in certain measured parameters like GRP78 and p-PERK/PERK. This discrepancy could stem from the complexity of the ER stress response, where compensatory pathways such as autophagy or mitochondrial

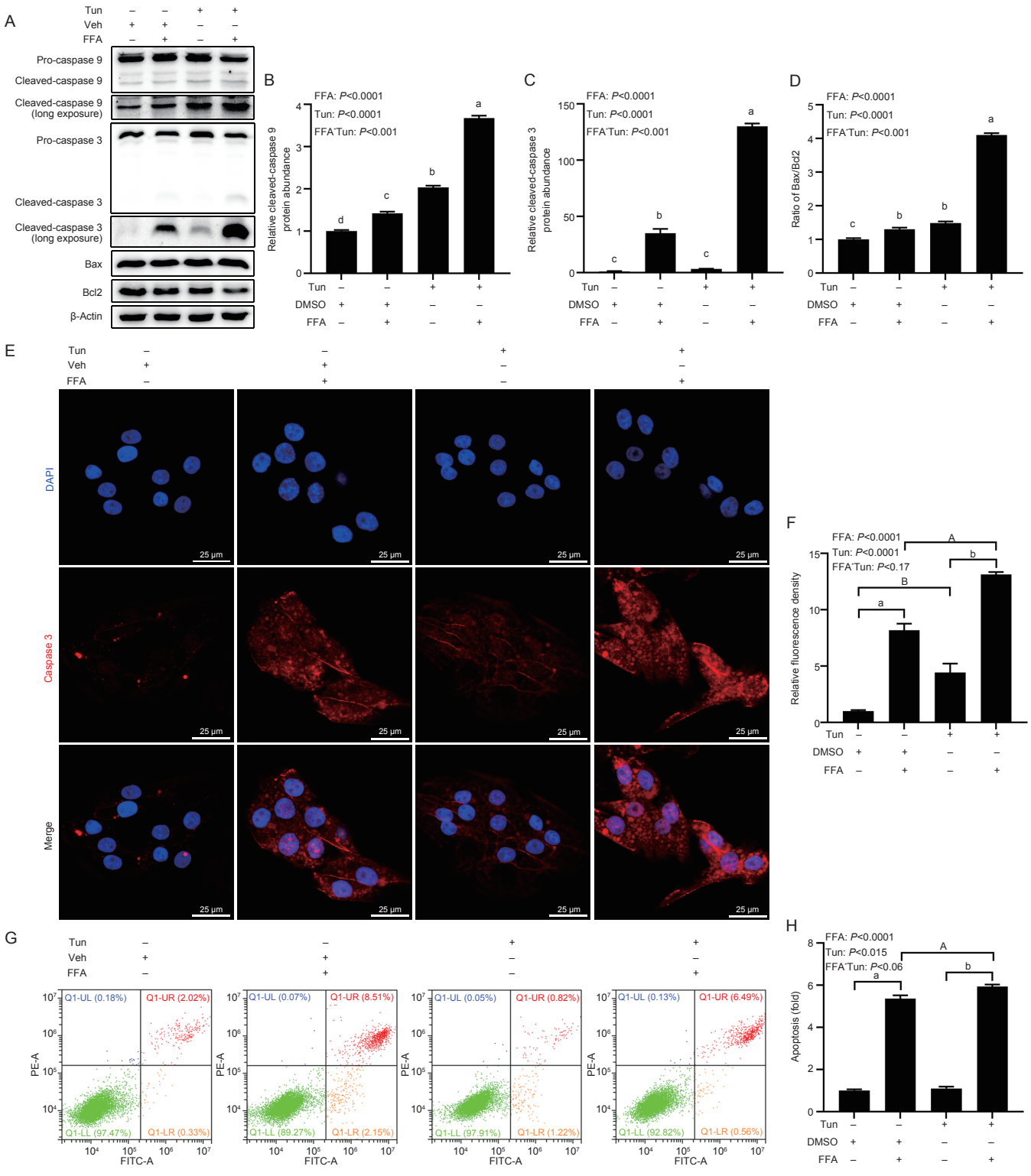


Fig. 4 Activation of endoplasmic reticulum (ER) stress aggravated free fatty acids (FFA)-induced apoptosis in MAC-T cells (Exp. 3). MAC-T cells were pretreated with DMSO or Tun for 12 h and treated with 0 or 1.2 mmol L^{-1} FFA in 2% BSA medium for another 24 h. A, Western blot image of caspase 9, caspase 3, BCL-2-associated X protein (Bax), B-cell lymphoma 2 (Bcl2), and β-actin. B and C, relative protein abundance of cleaved-caspase 9 (B) and cleaved-caspase 3 (C). D, ratio of Bax/Bcl2. E, representative image of immunofluorescence analysis of caspase 3. F, quantification of caspase 3 immunofluorescence. G, flow cytometric analysis of MAC-T cell apoptosis. PE-A indicates PI and FITC-A indicates Annexin V-FITC. Cells in Q1, Q2, Q3 and Q4 represent necrotic cells (negative for Annexin V-FITC and positive for PI) (Q1), late apoptotic cells (positive for both Annexin V-FITC and PI) (Q2), early apoptotic cells (positive for Annexin V-FITC and negative for PI) (Q3), and normal cells (negative for both Annexin V-FITC and PI) (Q4), respectively. H, quantification of cell apoptosis. Data are mean±SE (n=3). Different letters in single bars indicate a significant difference (P<0.05) determined by their interaction. Different uppercase letters in paired bars indicate significant differences (P<0.05) between Tun-treated and non-treated groups, as determined by the main effect of Tun. Different lowercase letters in paired bars indicate significant differences (P<0.05) between FFA-treated and non-treated groups, as determined by the main effect of FFA.

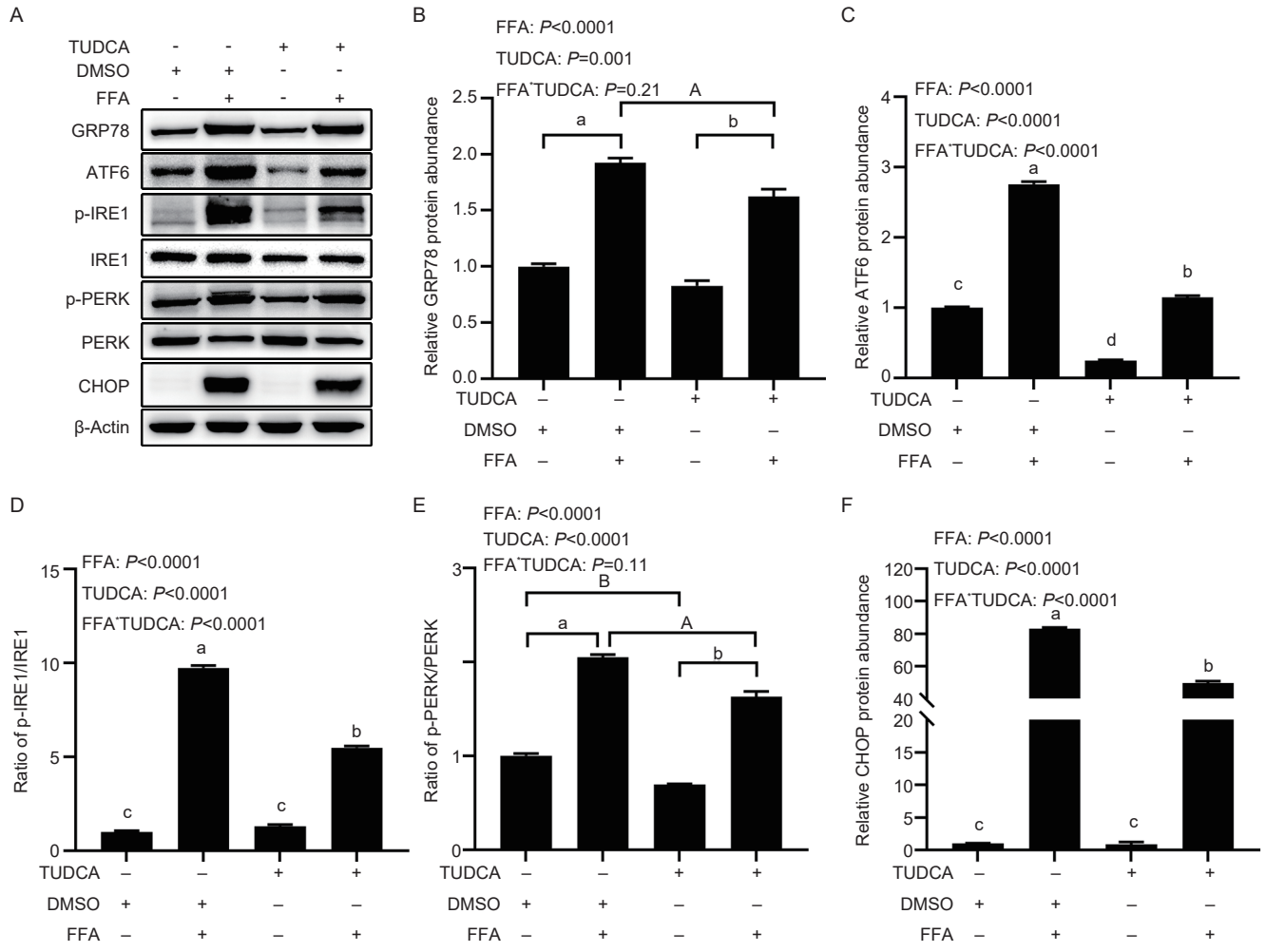


Fig. 5 Tauroursodeoxycholate (TUDCA) attenuated free fatty acids (FFA)-induced endoplasmic reticulum (ER) stress in MAC-T cells (Exp. 4). MAC-T cells were pretreated with DMSO or TUDCA for 12 h and treated with 0 or 1.2 mmol L^{-1} FFA in 2% BSA medium for another 24 h. A, Western blot image of GRP78, ATF6, p-IRE1, IRE1, p-PERK, PERK, CHOP, and β-actin. B, C and F, relative protein abundance of GRP78 (B), ATF6 (C) and CHOP (F). D and E, ratio of p-IRE1/IRE1 (D) and p-PERK/PERK (E). Data are mean±SE (n=3). Different letters in single bars indicate a significant difference (P<0.05) determined by their interaction. Different uppercase letters in paired bars indicate significant differences (P<0.05) between TUDCA-treated and non-treated groups, as determined by the main effect of TUDCA. Different lowercase letters in paired bars indicate significant differences (P<0.05) between FFA-treated and non-treated groups, as determined by the main effect of FFA.

dysfunction may have influenced the outcomes. Additionally, variations in cell responsiveness and FFA concentration could have introduced variability, leading to less significant interaction effects. Further investigation into these compensatory mechanisms and their role in modulating FFA-induced apoptosis is required to gain a more comprehensive understanding of the complex cellular response to metabolic stress.

Milk yield is the most important economic trait in dairy cows, the decrease of which in ketotic cows contributes to economic losses. Typically, the state of NEB due to the inability of energy consumed to meet energy requirements has been thought to be the main reason for lower milk yield in dairy cows with ketosis (Yue *et al.* 2022). However, in the strict sense, imbalances between apoptosis and proliferation of mammary epithelial cells are the basis of decreased of milk yield in cows undergoing metabolic disorders (Capuco *et al.* 2001; Sun *et al.* 2021). The excessive cellular apoptosis of mammary epithelial cells and lower milk yield observed in dairy cows with ketosis (Chang *et al.* 2023) served as impetus for studying in greater detail the regulatory mechanisms associated with metabolic stress-induced apoptosis in mammary gland.

The ER is an essential cellular organelle that is involved in protein homeostasis, and multiple factors such as physiological or pathological stressors cause an imbalance in ER homeostasis, resulting in ER stress. Excessive ER stress causes cell apoptosis even though it serves as a defense mechanism against external stress (Ceylan-Isik *et al.* 2011; Ge and Kao 2019). The process of ER stress is regulated by multiple molecular signaling pathways, with GRP78, a chaperone protein localized in the ER, being the main indicator of ER stress. Through a binding-release mechanism, its activity produces stress *via* three transmembrane ER stress sensors: PERK, ATF6, and IRE1 (Wang *et al.* 2015; Tawar *et al.* 2022). Upon ER stress,

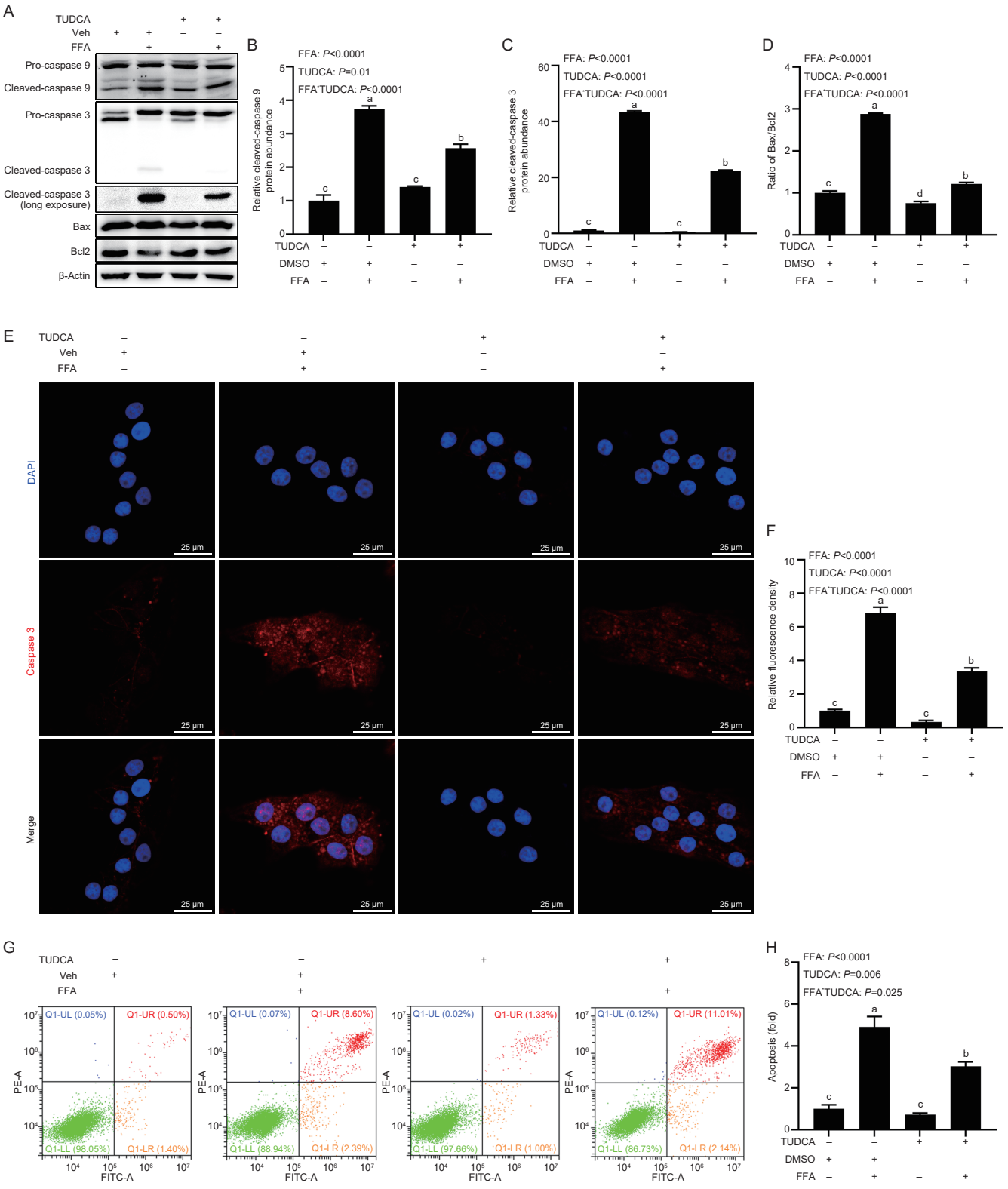


Fig. 6 Inhibition of endoplasmic reticulum (ER) stress attenuated apoptosis in MAC-T cells induced by free fatty acids (FFA) (Exp. 4). MAC-T cells were pretreated with DMSO or TUDCA for 12 h and treated with 0 or 1.2 mmol L^{-1} FFA in 2% BSA medium for another 24 h. A, Western blot image of caspase 9, caspase 3, Bax, Bcl2, and β-actin. B and C, relative protein abundance of cleaved-caspase 9 (B) and cleaved-caspase 3 (C). D, ratio of Bax/Bcl2. E, representative image of immunofluorescence analysis of caspase 3. F, quantification of caspase 3 immunofluorescence. G, flow cytometric analysis of MAC-T cell apoptosis. PE-A indicates PI and FITC-A indicates Annexin V-FITC. Cells in Q1, Q2, Q3 and Q4 represent necrotic cells (negative for Annexin V-FITC and positive for PI) (Q1), late apoptotic cells (positive for both Annexin V-FITC and PI) (Q2), early apoptotic cells (positive for Annexin V-FITC and negative for PI) (Q3), and normal cells (negative for both Annexin V-FITC and PI) (Q4), resepectively. H, quantification of cell apoptosis. Data are mean±SE (n=3). Different letters in single bars indicate a significant difference (P<0.05) determined by their interaction.

GRP78 is dissociated from PERK, ATF6, and IRE1 resulting in their activation and activation of the downstream signaling cascade including CHOP, an ER stress-related marker protein (Tan *et al.* 2022; Zhu *et al.* 2022). In the present study, the greater protein abundance of GRP78, ATF6, and CHOP along with the greater ratio of p-PERK/PERK and p-IRE1/IRE1 confirmed the existence of ER stress in mammary tissue of dairy cows with ketosis. Increased circulating concentrations of FFA in dairy cows with ketosis may be involved in this process (Luo *et al.* 2022). Previous studies have proven that FFA induce ER stress in hepatocytes of dairy cows (Huang *et al.* 2021). The increases in GRP78, ATF6, and CHOP protein abundance and the ratio of p-IRE1/IRE1 and p-PERK/PERK in mammary epithelial cells treated with FFA confirmed that the mammary glands of ketotic cows are direct target of FFA and its noxious effects.

In addition to maintaining cell homeostasis, the ER is also the center of *de novo* synthesis of various lipid species (Blomme *et al.* 2022; Jing *et al.* 2022). There is growing evidence that the unfolded protein response signaling pathway is the mechanism *via* which ER stress influences lipid metabolism (Basseri and Austin 2012; Ward *et al.* 2022). Milk fat secretion begins in the ER (McManaman *et al.* 2007; Han *et al.* 2020), at least in non-ruminant animals, ER stress is involved in the regulation of milk fat synthesis (Bobrovnikova-Marjon *et al.* 2008; Walker *et al.* 2022). One such possible mechanism is ER stress-induced insulin-induced gene-1 (INSIG-1) depletion. As a membrane protein residing in the ER, INSIG-1 is responsible for retention of the sterol regulatory element binding protein (SREBP) in the ER (Yang *et al.* 2002) thereby controlling milk fat synthesis (Carcangiu *et al.* 2013). At least in mouse liver, metabolic stress-induced ER stress contributes to SREBP-mediated lipid synthesis, which is associated with depletion of INSIG-1 (Zhang *et al.* 2012). Remarkably, palmitic acid activates the maturation of SREBP *via* reducing INSIG-1 in MAC-T cells, response that might promote milk fat synthesis (Chen L *et al.* 2021). Thus, the induction of ER stress by FFA in mammary epithelial cells may partly explain the greater milk fat content in ketotic dairy cows (Sun *et al.* 2021).

At least in non-ruminants, prolonged ER stress triggers apoptosis in various cell types (Haataja *et al.* 2008; Dalal *et al.* 2012; Menzie-Suderam *et al.* 2020). The ER stress-related apoptosis also has been reported in bovine endometrial epithelial cells and trophoblast cells (Chen W *et al.* 2021; Yuan *et al.* 2023). Because of the association between ER stress and apoptosis, and the markers of ER stress in this study corresponded with an increase in apoptosis in our previous study (Chang *et al.* 2023), we speculate that metabolic-induced ER stress might contribute to apoptosis in the mammary gland of dairy cows with ketosis.

Uncontrolled and prolonged ER stress can lead to cell apoptosis by activating downstream apoptosis-related signaling molecules (Walter and Ron 2011). The molecule Tun induces ER stress by blocking the first step of N-linked glycoprotein synthesis (You *et al.* 2018). In the present study, the increase in GRP78, ATF6, and CHOP protein abundance and the ratio of p-PERK/PERK and p-IRE1/IRE1 after Tun pretreatment confirmed previous data demonstrating that it activated ER stress *via* promoting ER transmembrane protein activation and dissociation from GRP78 (Bull and Thiede 2012; Guo *et al.* 2017). Furthermore, the increase in GRP78, ATF6, and CHOP protein levels along with the increases in ratio of p-IRE1/IRE1 and p-PERK/PERK indicated that Tun pretreatment aggravated the ER stress in bovine mammary epithelial cells induced by FFA.

Signaling through ER stress sensors could trigger apoptosis during prolonged ER stress (van der Kallen *et al.* 2009). Besides being an ER stress downstream marker, CHOP is the most important transcription factor in regulating ER stress-dependent apoptosis (Wu *et al.* 2021). The CHOP protein directly or indirectly participates in activation of caspase 9, which in turn cleaves the executioner caspase-3 and ultimately induces apoptosis (Mimura *et al.* 2012; Marzuca-Nassr *et al.* 2021). The pro-apoptotic protein Bax combines with Bcl2 to form a dimer leading to Bcl-2 inactivation, thereby promoting apoptosis. As such, the ratio of Bcl2 and Bax reflects the status of apoptosis (Li *et al.* 2021). In this study, the greater cleaved-caspase 9 and cleaved-caspase 3 protein abundance and the ratio of Bax/Bcl2 after FFA and Tun co-treatment suggested that Tun aggravated the FFA-activation of apoptotic process. The increase in number of apoptotic cells further corroborated that activation of ER stress aggravated the FFA-induced apoptosis in bovine mammary epithelial cells. Based on these results, we hypothesized that FFA-induced ER stress might contribute to apoptosis of mammary epithelial cells in mammary gland of dairy cows with ketosis.

The specific mechanisms whereby ER stress mediated apoptosis of bovine mammary epithelial cells is highly complex and may depend in an extra interplay with other signaling pathways. Notably, from a regulatory standpoint, calcium imbalance in cells due to ER stress might trigger apoptosis (Urra *et al.* 2013; Banerjee *et al.* 2017). The Ca^{2+} release system in the ER plays a crucial role in the ER-mitochondrial-Ca^{2+} cycle (Staats *et al.* 2016), and disturbance of this process could lead to mitochondrial ROS generation and depolarization of inner mitochondrial membrane (Duchen 1999; Kim and Kim 2018). In our previous study we observed that excessive Ca^{2+} uptake by mitochondria of bovine mammary epithelial cells cause mitochondrial depolarization and ROS production (Sun *et al.* 2023), with ROS subsequently contributing to FFA-mediated apoptosis (Chang *et al.* 2023). Together with the findings from our previous study, the present results suggested the possibility that Ca^{2+} released from the ER due to metabolic stress-induced stress is taken up by mitochondria, stimulating mitochondrial ROS production and further contributes to apoptosis in mammary cells. The actual impact of Ca^{2+} release from the ER on cell apoptosis merits further studies.

Inhibition of ER stress mitigates ER-associated apoptosis through regulating caspase-dependent intrinsic apoptosis pathways (Zhong *et al.* 2021). TUDCA is a small-molecule inhibitor of ER stress and can attenuate ER stress induced by metabolic disorders in mice (Wang *et al.* 2018). The lower protein abundance of CHOP, ATF6, and GRP78 and the ratio of p-IRE1/IRE1 and p-PERK/PERK in FFA and TUDCA co-treated cells confirmed that FFA-induced ER stress was

effectively attenuated by the administration of TUDCA. The lack of change in the protein abundance of CHOP and GRP78 and the ratio of p-IRE1/IRE1 after treatment alone with TUDCA is noteworthy. However, a similar response was reported in a study in which TUDCA was shown to attenuate obesity-induced ER stress without affecting these protein markers alone (Ceylan-Isik *et al.* 2011).

Inhibition of ER stress *in vitro* reduced apoptosis by suppressing the activation of caspase in mice (Montague *et al.* 2014), a response that agrees with the finding that TUDCA was effective in attenuating protein abundance of cleaved-caspase 9, cleaved-caspase3, and the ratio of Bax/Bcl2 in bovine mammary epithelial cells after FFA challenge. In addition, the attenuation in the number of apoptotic cells induced by FFA when ER stress was dampened by TUDCA suggested that a key mediator of FFA on apoptosis in mammary epithelial cells is the ER stress. These results are supported by earlier studies demonstrating that FFA induce ER stress (Kumar *et al.* 2021), and that inhibition of ER stress is an effective protective mechanism against metabolic stress-mediated apoptosis (Gundamaraju *et al.* 2018; Yang *et al.* 2018).

However, this study has certain limitations that need to be addressed. A notable limitation is the lack of direct measurements of caspase-12 activity. Caspase-12 is anchored to the ER membrane, where it plays a crucial role in ER-stress-induced apoptosis. Upon activation, caspase-12 triggers a cascade that ultimately results in the activation of caspase-3, which serves as the executioner caspase responsible for the final stages of apoptosis. Although our findings offer valuable insights into the effects of TUDCA on caspase-3, a more comprehensive understanding of the apoptotic pathway could be obtained by including data on caspase-12. Future research should focus on exploring the interaction between TUDCA and caspase-12 in greater detail to fully elucidate the mechanisms of ER-mediated apoptosis. Another significant limitation is that the study was conducted exclusively *in vitro*, which restricts the ability to fully extrapolate the findings to *in vivo* conditions. To confirm the effectiveness of ER stress inhibitors such as TUDCA, further research involving *in vivo* trials with dairy cows is essential. Despite this limitation, our research contributes to the growing body of evidence supporting the anti-apoptotic effects of ER stress inhibition in the mammary glands of dairy cows. Future research in this area, particularly studies incorporating caspase-12 analysis, will be crucial for developing more effective therapeutic strategies for diseases related to ER-stress-induced apoptosis in dairy cows with ketosis.

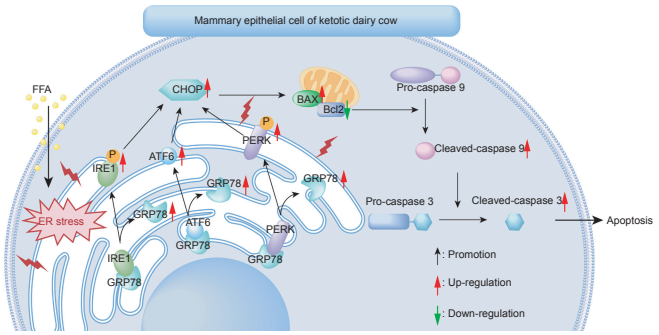


Fig. 7 High concentrations of free fatty acids (FFA) as a result of metabolic stress lead to apoptosis of mammary epithelial cell through excessive endoplasmic reticulum (ER) stress in the mammary gland of dairy cows with ketosis.

5. Conclusion

In conclusion, high concentrations of FFA as a result of metabolic stress lead to apoptosis of mammary epithelial cell through excessive ER stress in the mammary gland of ketotic dairy cows. As such, treatment with ER stress inhibitors such as TUDCA may offer a promising therapeutic approach for cows undergoing metabolic disorders that elevate circulating FFA such as ketosis. Future research should focus on conducting trials in dairy cows to confirm the effectiveness of ER stress inhibitor and assess their practical application in managing ER stress-related conditions in real-world settings. This step is crucial for translating our findings into effective strategies for improving dairy cattle health and productivity.

Acknowledgements

This work was supported by the National Key R&D Program of China (2023YFD1802100), the National Natural Science Foundation of China (32072931) and the Earmarked Fund for CARS36, China.

Declaration of competing interest

The authors declare that they have no conflict of interest.

Declaration of generative AI and AI-assisted technologies in the writing process

The authors declare that they did not use AI in the preparation and writing of this manuscript.

Ethical approval

The Heilongjiang Bayi Agricultural University Laboratory Animal Center's Animal Welfare and Ethics Committee approved the animal experiments.

References

Banerjee K, Keasey M P, Razskazovskiy V, Visavadiya N P, Jia C, Hagg T. 2017. Reduced FAK-STAT3 signaling contributes to ER stress-induced mitochondrial dysfunction and death in endothelial cells. *Cellular Signalling*, **36**, 154–162.

Basseri S, Austin R C. 2012. Endoplasmic reticulum stress and lipid metabolism: Mechanisms and therapeutic potential. *Biochemistry Research International*, **2012**, 841362.

Bauer E A, Jagusiak W. 2022. The use of multilayer rerceptron artificial neural networks to detect dairy cows at risk of ketosis. *Animals* (Basel), **12**, 332.

Blomme A, Peter C, Mui E, Rodriguez Blanco G, An N, Mason L M, Jamieson L E, McGregor G H, Lilla S, Ntala C, Patel R, Thiry M, Kung SHY, Leclercq M, Ford C A, Rushworth L K, McGarry D J, Mason S, Repiscak P, Nixon C, *et al.* 2022. THEM6-mediated reprogramming of lipid metabolism supports treatment resistance in prostate cancer. *EMBO Molecular Medicine*, **14**, e14764.

Bobrovnikova-Marjon E, Hatzivassiliou G, Grigoriadou C, Romero M, Cavener D R, Thompson C B, Diehl J A. 2008. PERK-dependent regulation of lipogenesis during mouse mammary gland development and adipocyte differentiation. *Proceedings of the National Academy of Sciences of the United States of America*,

105, 16314–16319.
Bull V H, Thiede B. 2012. Proteome analysis of tunicamycin-induced ER stress. *Electrophoresis*, **33**, 1814–1823.
Capuco A V, Wood D L, Baldwin R, McLeod K, Paape M J. 2001. Mammary cell number, proliferation, and apoptosis during a bovine lactation: Relation to milk production and effect of bST. *Journal of Dairy Science*, **84**, 2177–2187.
Carcangiu V, Mura M C, Daga C, Luridiana S, Bodano S, Sanna G A, Diaz M L, Cosso G. 2013. Association between SREBP-1 gene expression in mammary gland and milk fat yield in Sarda breed sheep. *Meta Gene*, **1**, 43–49.
Ceylan-Isik A F, Sreejayan N, Ren J. 2011. Endoplasmic reticulum chaperon tauroursodeoxycholic acid alleviates obesity-induced myocardial contractile dysfunction. *Journal of Molecular and Cellular Cardiology*, **50**, 107–116.
Chang R, Jia H, Dong Z, Xu Q, Liu L, Majigsuren Z, Batbaatar T, Xu C, Yang Q, Sun X. 2023. Free fatty acids induce apoptosis of mammary epithelial cells of ketotic dairy cows *via* the Mito-ROS/NLRP3 signaling pathway. *Journal of Agricultural and Food Chemistry*, **71**, 12645–12656.
Chang R, Sun X, Jia H, Xu Q, Dong Z, Tang Y, Luo S, Jiang Q, Loor J J, Xu C. 2022. Inhibiting nuclear factor erythroid 2 related factor 2-mediated autophagy in bovine mammary epithelial cells induces oxidative stress in response to exogenous fatty acids. *Journal of Animal Science and Biotechnology*, **13**, 48.
Chen L, Lengi A J, Corl B A. 2021. The inhibitory effect of *trans*-10, *cis*-12 conjugated linoleic acid on sterol regulatory element binding protein-1 activation in bovine mammary epithelial cells involved reduced proteasomal degradation of insulin-induced gene-1. *Journal of Dairy Science*, **104**, 11306–11316.
Chen W, Wu J, Zhan S, Lu X. 2021. Honokiol inhibits endoplasmic reticulum stress-associated lipopolysaccharide-induced inflammation and apoptosis in bovine endometrial epithelial cells. *Experimental and Therapeutic Medicine*, **22**, 1476.
Dalal S, Foster C R, Das B C, Singh M, Singh K. 2012. Beta-adrenergic receptor stimulation induces endoplasmic reticulum stress in adult cardiac myocytes: Role in apoptosis. *Molecular and Cellular Biochemistry*, **364**, 59–70.
Duchen M R. 1999. Contributions of mitochondria to animal physiology: From homeostatic sensor to calcium signalling and cell death. *Journal of Physiology*, **516**, 1–17.
Ge R, Kao C. 2019. Cell surface GRP78 as a death receptor and an anticancer drug target. *Cancers*, **11**, 1787.
Gu F, Miao C, Jiang L, Wang D, Liu H, Liu J. 2021. Dietary supplementation with N-carbamoylglutamate initiated from the prepartum stage improves lactation performance of postpartum dairy cows. *Animal Nutrition*, **7**, 232–238.
Gundamaraju R, Vemuri R, Chong W C, Myers S, Norouzi S, Shastri M D, Eri R. 2018. Interplay between endoplasmic reticulars stress and survivin in colonic epithelial cells. *Cells*, **7**, 171.
Guo Q, Li H, Liu J, Xu L, Yang L, Sun Z, Zhou B. 2017. Tunicamycin aggravates endoplasmic reticulum stress and airway inflammation *via* PERK-ATF4-CHOP signaling in a murine model of neutrophilic asthma. *Journal of Asthma*, **54**, 125–133.
Haataja L, Gurlo T, Huang C J, Butler P C. 2008. Many commercially available antibodies for detection of CHOP expression as a marker of endoplasmic reticulum stress fail specificity evaluation. *Cell Biochemistry and Biophysics*, **51**, 105–107.
Han L, Zhang M, Xing Z, Coleman D N, Liang Y, Loor J J, Yang G. 2020. Knockout of butyrophilin subfamily 1 member A1 (BTN1A1) alters lipid droplet formation and phospholipid composition in bovine mammary epithelial cells. *Journal of Animal Science and Biotechnology*, **11**, 72.
Huang Y, Zhao C, Liu Y, Kong Y, Tan P, Liu S, Zeng F, Yuan Y, Li X, Liu G, Zhao B, Wang J. 2021. NEFA promotes autophagosome formation through modulating PERK signaling pathway in bovine hepatocytes. *Animals* (Basel), **11**, 3400.
Jing J, Yin S, Liu Y, Liu Y, Wang L, Tang J, Jia G, Liu G, Tian G, Chen X, Cai J, Kang B, Zhao H. 2022. Hydroxy selenomethionine alleviates hepatic lipid metabolism disorder of pigs induced by dietary oxidative stress *via* relieving the endoplasmic reticulum stress. *Antioxidants* (Basel), **11**, 552.
van der Kallen C J, van Greevenbroek M M, Stehouwer C D, Schalkwijk C G. 2009. Endoplasmic reticulum stress-induced apoptosis in the development of diabetes: Is there a role for adipose tissue and liver? *Apoptosis*, **14**, 1424–1434.
Kim C Kim B. 2018. Anti-cancer natural products and their bioactive compounds inducing ER stress-mediated apoptosis: A review. *Nutrients*, **10**, 1021.
Kumar V, Xin X, Ma J, Tan C, Osna N, Mahato R I. 2021. Therapeutic targets, novel drugs, and delivery systems for diabetes associated NAFLD and liver fibrosis. *Advanced Drug Delivery Reviews*, **176**, 113888.
Li B, Hock A, Wu R Y, Minich A, Botts S R, Lee C, Antounians L, Miyake H, Koike Y, Chen Y, Zani A, Sherman P M, Pierro A. 2019. Bovine milk-derived exosomes enhance goblet cell activity and prevent the development of experimental necrotizing enterocolitis. *PLoS ONE*, **14**, e0211431.
Li M, Zhang B, Yin Y, Wen J, Wang J, He Y, Jiang Q, Loor J J, Wang S, Yang W, Xu C. 2022. Intracellular Ca^{2+} signaling and calcium release-activated calcium modulator ORAI1 are associated with $CD4^{+}$ T lymphocytes in dairy cows. *Frontiers in Immunology*, **13**, 835936.
Li Y, Zhang W, Liu M, Zhang Q, Lin Z, Jia M, Liu D, Lin L. 2021. Imbalance of autophagy and apoptosis induced by oxidative stress may be involved in thyroid damage caused by sleep deprivation in rats. *Oxidative Medicine and Cellular Longevity*, **2021**, 5645090.
Lu J, Li Y, Gong S, Wang J, Lu X, Jin Q, Lu B, Chen Q. 2022. Ciclopirox targets cellular bioenergetics and activates ER stress to induce apoptosis in non-small cell lung cancer cells. *Cell Communication and Signaling*, **20**, 37.
Luo Z, Huang Y, Ma L, Jiang J, Luo Q, Yang Z, Yong K, Shen L, Yu S, Yao X, Tao J, Cao S. 2022. Untargeted metabolomics reveals metabolic stress alleviation by prepartum exercise in transition dairy cows. *Metabolites*, **12**, 309.
Marzuca-Nassr G N, Kuwabara W M T, Vitzel K F, Murata G M, Torres R P, Mancini-Filho J, Alba-Loureiro T C, Curi R. 2021. Endoplasmic reticulum stress and autophagy markers in soleus muscle disuse-induced atrophy of rats treated with fish oil. *Nutrients*, **13**, 2298.
McManaman J L, Russell T D, Schaack J, Orlicky D J, Robenek H. 2007. Molecular determinants of milk lipid secretion. *Journal of Mammary Gland Biology and Neoplasia*, **12**, 259–268.
Menzie-Suderam J M, Modi J, Xu H, Bent A, Trujillo P, Medley K, Jimenez E, Shen J, Marshall M, Tao R, Prentice H, Wu J Y. 2020. Granulocyte-colony stimulating factor gene therapy as a novel therapeutics for stroke in a mouse model. *Journal of Biomedical Science*, **27**, 99.
Miles A M, McArt J A A, Lima S F, Neves R C, Ganda E. 2022. The association of hyperketonemia with fecal and rumen microbiota at time of diagnosis in a case-control cohort of early lactation cows. *BMC Veterinary Research*, **18**, 411.
Mimura N, Fulciniti M, Gorgun G, Tai Y T, Cirstea D, Santo L, Hu Y, Fabre C, Minami J, Ohguchi H, Kiziltepe T, Ikeda H, Kawano Y, French M, Blumenthal M, Tam V, Kertesz N L, Malyankar U M, Hokenson M, Pham T, *et al.* 2012. Blockade of XBP1 splicing by inhibition of IRE1alpha is a promising therapeutic option in multiple myeloma. *Blood*, **119**, 5772–5781.
Mo J, Ruan S, Yang B, Jin Y, Liu K, Luo X, Jiang H. 2023. A novel defined risk signature of endoplasmic reticulum stress-related genes for predicting the prognosis and immune infiltration status of ovarian cancer. *Journal of Zhejiang University Science B*, **24**, 64–77.
Montague K, Malik B, Gray A L, La Spada A R, Hanna M G, Szabadkai G, Greensmith L. 2014. Endoplasmic reticulum stress in spinal and bulbar muscular atrophy: A potential target for therapy. *Brain*, **137**, 1894–1906.
Montevecchio A B, Frota W, Merenda V R, Martin 3rd J G, Chebel R C. 2023. A randomized trial on the effects of heat stress abatement on environmental conditions and growth, feed efficiency, and concentration of metabolites of pre-weaned female Holstein calves. *Preventive Veterinary Medicine*, **213**, 105863.
Moslehi A, Komeili-Movahhed T, Ahmadian M, Ghoddoosi M, Heidari F. 2023. Chlorogenic acid attenuates liver apoptosis and inflammation in endoplasmic reticulum stress-induced mice. *Iranian Journal of Basic Medical Sciences*, **26**, 478–485.
Nasiri-Ansari N, Nikolopoulou C, Papoutsi K, Kyrou I, Mantzoros C S, Kyriakopoulos G, Chatzigeorgiou A, Kalotychou V, Randeva M S, Chatha K, Kontzoglou K, Kaltsas G, Papavassiliou A G, Randeva H S, Kassi E. 2021. Empagliflozin attenuates non-alcoholic fatty liver disease (NAFLD) in high fat diet fed $ApoE^{-/-}$ mice by activating

autophagy and reducing ER stress and apoptosis. *International Journal of Molecular Sciences*, **22**, 818.
NRC (National Research Council). 2021. *Nutrient Requirements of Dairy Cattle: Eighth Revised Edition*. The National Academies Press, Washington, DC.
Papandreou I, Verras M, McNeil B, Koong A C, Denko N C. 2015. Plant stilbenes induce endoplasmic reticulum stress and their anti-cancer activity can be enhanced by inhibitors of autophagy. *Experimental Cell Research*, **339**, 147–153.
Ruprechter G, Carriquiry M, Ramos J M, Pereira I, Ana M. 2011. Metabolic and endocrine profiles and reproductive parameters in dairy cows under grazing conditions: Effect of polymorphisms in somatotropic axis genes. *Acta Veterinaria Scandinavica*, **53**, 35.
Saun R J V. 2022. Nutritional requirements of dairy cattle. vol. 2022. In: MSD (Merck Sharp & Dohme) Veterinary Manual. Merck & Co., USA.
Van Soest P J, Robertson J B, Lewis B A. 1991. Methods for dietary fiber, neutral detergent fiber, and nonstarch polysaccharides in relation to animal nutrition. *Journal of Dairy Science*, **74**, 3583–3597.
Staats K A, Humblet-Baron S, Bento-Abreu A, Scheveneels W, Nikolaou A, Deckers K, Lemmens R, Goris A, Van Ginderachter J A, Van Damme P, Hisatsune C, Mikoshiba K, Liston A, Robberecht W, Van Den Bosch L. 2016. Genetic ablation of IP3 receptor 2 increases cytokines and decreases survival of SOD1G93A mice. *Human Molecular Genetics*, **25**, 3491–3499.
Sun X, Gao S, Luo S, Chang R, Jia H, Xu Q, Jiang Q, Loor J J, Xu C. 2023. Mitochondrial calcium uniporter regulator 1 (MCUR1) relieves mitochondrial damage induced by lipopolysaccharide by mediating mitochondrial Ca^{2+} homeostasis in bovine mammary epithelial cells. *Journal of Agricultural and Food Chemistry*, **71**, 7278–7288.
Sun X, Tang Y, Jiang C, Luo S, Jia H, Xu Q, Zhao C, Liang Y, Cao Z, Shao G, Loor J J, Xu C. 2021. Oxidative stress, NF-kappaB signaling, NLRP3 inflammasome, and caspase apoptotic pathways are activated in mammary gland of ketotic Holstein cows. *Journal of Dairy Science*, **104**, 849–861.
Sun X, Wang Y, Loor J J, Bucktrout R, Shu X, Jia H, Dong J, Zuo R, Liu G, Li X, Li X. 2019. High expression of cell death-inducing DFFA-like effector a (CIDEA) promotes milk fat content in dairy cows with clinical ketosis. *Journal of Dairy Science*, **102**, 1682–1692.
Tan Y, Zhang X, Zhou Y, Miao L, Xu B, Khan H, Wang Y, Yu H, Cheang W S. 2022. Panax notoginseng extract and total saponin suppress diet-induced obesity and endoplasmic reticulum stress in epididymal white adipose tissue in mice. *Chinese Medicine*, **17**, 75.
Tawar N, Banerjee B D, Madhu S V, Agrawal V, Gupta S. 2022. Association of organochlorine pesticides with genetic markers of endoplasmic reticulum stress in type 2 diabetes mellitus: A case-control study among the north-Indian population. *Frontiers in Endocrinology*, **13**, 841463.
Urra H, Dufey E, Lisbona F, Rojas-Rivera D, Hetz C. 2013. When ER stress reaches a dead end. *Biochimica et Biophysica Acta*, **1833**, 3507–3517.
Waldherr S M, Strovas T J, Vadset T A, Liachko N F, Kraemer B C. 2019. Constitutive XBP-1s-mediated activation of the endoplasmic reticulum unfolded protein response protects against pathological tau. *Nature Communications*, **10**, 4443.
Walker R E, Ma L, Li C, Ying Y, Harvatine K J. 2022. TRB3 deletion has a limited effect on milk fat synthesis and milk fat depression in C57BL/6N mice. *Current Developments in Nutrition*, **6**, nzab142.
Walter P, Ron D. 2011. The unfolded protein response: From stress pathway to homeostatic regulation. *Science*, **334**, 1081–1086.
Wang W, Zhao J, Gui W, Sun D, Dai H, Xiao L, Chu H, Du F, Zhu Q, Schnabl B, Huang K, Yang L, Hou X. 2018. Tauroursodeoxycholic acid inhibits intestinal inflammation and barrier disruption in mice with non-alcoholic fatty liver disease. *British Journal of Pharmacology*, **175**, 469–484.
Wang X, Lin P, Yin Y, Zhou J, Lei L, Zhou X, Jin Y, Wang A. 2015. Brucella suis vaccine strain S2-infected immortalized caprine endometrial epithelial cell lines induce non-apoptotic ER-stress. *Cell Stress & Chaperones*, **20**, 399–409.
Wang X, Song Q. 2018. Mst1 regulates post-infarction cardiac injury through the JNK-Drp1-mitochondrial fission pathway. *Cellular & Molecular Biology Letters*, **23**, 21.
Ward C P, Peng L, Yuen S, Chang M, Karapetyan R, Nyangau E, Mohammed H, Palacios H, Ziari N, Joe L K, Frakes A E, Dandan M, Dillin A, Hellerstein M K. 2022. ER unfolded protein response in liver *in vivo* is characterized by reduced, not increased, *de novo* lipogenesis and cholesterol synthesis rates with uptake of fatty acids from adipose tissue: Integrated gene expression, translation rates and metabolic fluxes. *International Journal of Molecular Sciences*, **23**, 1073.
Wu J, Yang F, Zhang X, Chen G, Zou J, Yin L, Yang D. 2021. Hydrogen sulfide inhibits endoplasmic reticulum stress through the GRP78/mTOR pathway in rat chondrocytes subjected to oxidative stress. *International Journal of Molecular Medicine*, **47**, 34.
Xu Q, Zhang H, Wang S, Qin C, Lu Y. 2021. Constitutive expression of spliced XBP1 causes perinatal lethality in mice. *Genesis*, **59**, e23420.
Yang L, Guan G, Lei L, Lv Q, Liu S, Zhan X, Jiang Z, Gu X. 2018. Palmitic acid induces human osteoblast-like Saos-2 cell apoptosis *via* endoplasmic reticulum stress and autophagy. *Cell Stress & Chaperones*, **23**, 1283–1294.
Yang T, Espenshade P J, Wright M E, Yabe D, Gong Y, Aebersold R, Goldstein J L, Brown M S. 2002. Crucial step in cholesterol homeostasis: Sterols promote binding of SCAP to INSIG–1, a membrane protein that facilitates retention of SREBPs in ER. *Cell*, **110**, 489–500.
You S, Li W, Guan Y. 2018. Tunicamycin inhibits colon carcinoma growth and aggressiveness *via* modulation of the ERK-JNK-mediated AKT/mTOR signaling pathway. *Molecular Medicine Reports*, **17**, 4203–4212.
Yuan N, Song Q, Jin Y, Zhang Z, Wu Z, Sheng X, Qi X, Xing K, Xiao L, Wang X. 2023. Replication of standard bovine viral diarrhea strain OregonC24Va induces endoplasmic reticulum stress-mediated apoptosis of bovine trophoblast cells. *Cell Stress & Chaperones*, **28**, 49–60.
Yue K, Pu X, Loor J J, Jiang Q, Dong J, Shen T, Li G, Gao W, Lei L, Du X, Song Y, Liu G, Li X. 2022. Impaired autophagy aggravates oxidative stress in mammary gland of dairy cows with clinical ketosis. *Journal of Dairy Science*, **105**, 6030–6040.
Zhang C, Chen X, Zhu R M, Zhang Y, Yu T, Wang H, Zhao H, Zhao M, Ji Y L, Chen Y H, Meng X H, Wei W, Xu D X. 2012. Endoplasmic reticulum stress is involved in hepatic SREBP-1c activation and lipid accumulation in fructose-fed mice. *Toxicology Letters*, **212**, 229–240.
Zhao C, Yin S, Dong Y, Guo X, Fan L, Ye M, Hu H. 2013. Autophagy-dependent EIF2AK3 activation compromises ursolic acid-induced apoptosis through upregulation of MCL1 in MCF-7 human breast cancer cells. *Autophagy*, **9**, 196–207.
Zhong Y, Jin C, Han J, Zhu J, Liu Q, Sun D, Xia X, Peng X. 2021. Inhibition of ER stress attenuates kidney injury and apoptosis induced by 3-MCPD *via* regulating mitochondrial fission/fusion and Ca^{2+} homeostasis. *Cell Biology and Toxicology*, **37**, 795–809.
Zhu Q J, Zhang L, Lyu S Y, Cui Z J, Jiang E S, Wang J. 2022. Protective limb remote ischemic post-conditioning against high-intraocular-pressure-induced retinal injury in mice. *International Journal of Ophthalmology*, **15**, 560–567.
Zhu Y, Guan Y, Loor J J, Sha X, Coleman D N, Zhang C, Du X, Shi Z, Li X, Wang Z, Liu G, Li X. 2019. Fatty acid-induced endoplasmic reticulum stress promoted lipid accumulation in calf hepatocytes, and endoplasmic reticulum stress existed in the liver of severe fatty liver cows. *Journal of Dairy Science*, **102**, 7359–7370.

Executive Editor-in-Chief Xugang Luo
Managing Editor Han Zhang